 CMES, vol.28, no.2, pp.77-93, 2008

Improving the Ill-conditioning of the Method of Fundamental Solutions for 2D Laplace Equation

Chein-Shan Liu[1]

Abstract: The method of fundamental solutions (MFS) is a truly meshless numerical method widely used in the elliptic type boundary value problems, of which the approximate solution is expressed as a linear combination of fundamental solutions and the unknown coefficients are determined from the boundary conditions by solving a linear equations system. However, the accuracy of MFS is severely limited by its ill-conditioning of the resulting linear equations system. This paper is motivated by the works of Chen, Wu, Lee and Chen (2007) and Liu (2007a). The first paper proved an equivalent relation of the Trefftz method and MFS for circular domain, while the second proposed a modified Trefftz method (MTM). We first prove an equivalent relation of MTM and MFS for arbitrary plane domain. Due to the well-posedness of MTM, we can alleviate the ill-conditioning of MFS through a new linear equations system of the modified MFS (MMFS). In doing so we can raise the accuracy of MMFS over four orders more than the original MFS. Numerical examples indicate that the MMFS can attain highly accurate numerical solutions with accuracy over the order of 10^{-10}. The present method is fully not similar to the preconditioning technique as used to solve the ill-conditioned linear equations system.

Keyword: Laplace equation, Modified Trefftz method, Collocation method, Method of fundamental solutions, Modified MFS (MMFS).

[1] Department of Mechanical & Mechatronic Engineering, Department of Harbor & River Engineering, Taiwan Ocean University, Keelung, Taiwan. E-mail: csliu@mail.ntou.edu.tw

1 Introduction

For a complicated shape of the problem domain the standard numerical methods like as FEM and BEM required a large number of nodes and elements to match the geometrical shape. In order to overcome these deficiencies, the meshless numerical methods are proposed, which are meshes free and only boundary nodes are necessary. Among these efforts, the meshless local boundary integral equation (LBIE) method is proposed by Atluri and Shen (1999), and the meshless local Petrov-Galerkin (MLPG) method is proposed by Atluri, Kim and Cho (2002). Both methods use local weak forms and the integrals can be easily evaluated over circles in 2D problems and spheres in 3D problems.

Algorithms based on the discretizations of integral equations are often convenient for problems with complicated domains because of the reduced complexity of discretization when compare them with the competing approach such as FEM. For this reason there were many researchers devoted to overcome the difficulties appeared in the boundary integral equations. At the first, Landweber and Macagno (1969) have proposed a method to get rid of the singularity by substracting a function from the integrand so that the kernel becomes non-singular, and then adding back an accurate integration of the function to the integral equation. This method was modified and referred to as the non-singular boundary integral method by Hwang and Huang (1998) and Fan and Young (2002), or the desingularized boundary integral method by Chuang (1999). Recently, Liu (2007b) has developed a meshless regularized integral equation method for the Laplace equation in arbitrary plane domain, and Liu (2007c) extended these results to the Laplace problem defined in a doubly-

connected region. The basic idea in these two papers is by using the second-kind Fredholm integral equations on artificial circles, and using the degenerate kernels instead of the singular kernels.

Another way to avoid the singularity was proposed by Cao, Schultz and Beck (1991), Lalli (1997) and Zhang, Yeo, Khoo and Chong (1999), which moves the computing nodes away from the boundary and outside the real domain of the problem. Even, this new approach can overcome the difficulties of singular integrals, it has another problem of ill-posedness due to the appearence of the first-kind Fredholm integral equations. Therefore, Young (1999) and Young, Chen and Lee (2005) have applied the desingularized boundary integral equation method to the potential problems. In these approaches the source points are located in the real boundary, and they regularized the singular integrals by using the Gauss' flux theorem.

The Trefftz method is truly meshless, since it can be implemented without needing either domain or surface meshing. However, it is known that the Trefftz method is severely ill-posed when the number of bases is increased. In order to overcome this ill-posedness, Liu (2007a) has proposed a modified Trefftz method (MTM) by including the characteristic length of the problem domain into the bases. Remarkably, the MTM performs much better than the original Trefftz method. Liu (2007d) has proposed by using the MTM to calculate the Laplace problems under mixed-boundary conditions. Because the ill-posedness of the conventional Trefftz method is overcome by the new method, it can be even applied on the singular problem with a high accuracy never seen before. Liu (2007e) has employed the same idea to modify the direct Trefftz method for the two-dimensional potential problem, and Liu (2008) used this idea to develop a highly accurate numerical method to calculate the Laplace equation in doubly-connected domains.

On the other hand, the method of fundamental solutions (MFS) is also a truly meshless numerical method popularly used in the elliptic type boundary value problems, of which the approximate solution is expressed as a linear combination of fundamental solutions of the considered partial differential equation. The MFS is one sort of the Trefftz method because the approximate solutions are obtained through a linear combination of exact solutions of the underlying equation. In order to distinct it from the above mentioned T-Trefftz method, some authors also called the MFS as the F-Trefftz method. The coefficients of linear combination as that for the T-Trefftz method are determined from the boundary conditions. The MFS is very easy to implement and it avoids the integrations on the boundary. Because the MFS is an inherently meshless boundary method and has exponential convergence property for smooth solutions, it has been used extensively for solving the Laplace equation [Fairweather (1998); Saavedra (2003)]. The error estimates, stability and convergence analyses of the MFS for the Laplace equation in disk are carried out by Bogomolny (1985) and Smyrlis and Karageorghis (2001). The MFS has a broad application in engineering computations, for example, Cho, Golberg, Muleshkov and Li (2004), Hon and Wei (2005), Young, Chen and Lee (2005), Young and Ruan (2005), and Young, Tsai, Lin and Chen (2006).

Similarly the MFS has the problem that the resulting linear equations system may become highly ill-conditioned when the number of source points is increased [Golberg (1996)] or when the distances of source points are increased [Chen (2006)]. The convergence analysis of MFS has demonstrated that the approximation improves when the source radius tends to infinity; see. e.g., Smyrlis and Karageorghis (2004). Nevertheless, a commonly encountered problem is its poor accuracy as the source radius is increased to a large vaule in the numerical computation. The ill-conditioning of the MFS makes the accurate approximation by the numerical solutions of the boundary value problems extremely difficult.

An improved method than the MFS is the so-called boundary knot method [Chen (2002); Jin (2006)] or the boundary collocation method [Chen (2002a); Chen (2002b)]. Instead of the singular fundamental solutions, these methods employed the non-singular kernels to evaluate the homogeneous solutions. However, as pointed out

by Young, Chen and Lee (2005) the introduction of non-singular kernels as the radial basis functions may jeopardize the accuracy of solutions as compared with the MFS.

Tsai, Lin, Young and Atluri (2006) have proposed a numerical procedure to locate the sources of the MFS. In their numerical experiments, higher condition numbers and smaller errors are observed when the sources are located farther in a proper way. They proposed a practical procedure to locate the sources in the use of MFS for various time independent operators. The procedure is developed through some systematic numerical experiments for relations among the accuracy, condition number, and source positions in different shapes of computational domains. By numerical experiments, they found that good accuracy can be achieved when the condition number approaches the limit of equation solver.

Then, Young, Chen, Chen and Kao (2007) have proposed a modified method of fundamental solutions for solving the Laplace problems, which implements the singular fundamental solutions to evaluate the solutions, and it can locate the source points on the real boundary as contrasted to the conventional MFS. Therefore, the major difficulty of the coincidence of the source and collocation points in the conventional MFS is thereby overcome, and the ill-posed nature of the conventional MFS disappears.

This paper will re-formulate the MFS in a new setting, different from that in the above cited paper. A significant improvement of the ill-conditioning associated with the linear equations system of MFS is possible. In Section 2 we summarize the MTM, which takes the characteristic length into account. In Section 3 we derive a collocation numerical method of the new version. The MFS is briefly summarized in Section 4, and then in Section 5 we derive a new relation between the MTM and the MFS for a circular boundary by using the concept of degenerate kernel. Those results are extended in Section 6 to arbitrary plane domain, and thus we can propose a new method for a big improvement of the MFS. In Section 7 we use some numerical examples to test and compare the numerical methods of MFS, normalized MFS (NMFS), modified MFS (MMFS) as well as the modified Trefftz method (MTM). Finally, we draw some conclusions in Section 8.

2 A modified Trefftz method

The Trefftz method automatically satisfies the governing equation and leaves the unknown coefficients determined by satisfying the boundary conditions [Kita and Kamiya (1995); Kita, Kamiya and Iio (1999)]. Recently, Li, Lu, Huang and Cheng (2006) gave a very comprehensive comparison of the Trefftz, collocation and other boundary methods. They concluded that the collocation Trefftz method is the simplest algorithm and provides the most accurate solution with the best numerical stability.

In this paper we begin with a new MTM proposed by Liu (2007a) to solve the Dirichlet problem under boundary condition specified on a non-circular boundary as shown in Fig. 1:

$$\Delta u = u_{rr} + \frac{1}{r}u_r + \frac{1}{r^2}u_{\theta\theta} = 0, \quad r < \rho \ \text{ or } \ r > \rho, \quad 0 \le \theta \le 2\pi, \tag{1}$$

$$u(\rho,\theta) = h(\theta), \quad 0 \le \theta \le 2\pi, \tag{2}$$

where $h(\theta)$ is a given function, and $r = \rho(\theta)$ is a given contour describing the boundary shape of the interior or exterior domain. The boundary contour $\partial\Omega$ of the problem domain Ω in polar coordinates is described by $\partial\Omega = \{(r,\theta)|r = \rho(\theta),\ 0 \le \theta \le 2\pi\}$. For exterior problem Ω is unbounded, and Ω is bounded for interior problem. The complement of Ω is denoted by $\Omega^c = \mathbb{R}^2/\overline{\Omega}$.

We replace Eq. (2) by the following boundary condition:

$$u(R_0,\theta) = f(\theta), \quad 0 \le \theta \le 2\pi, \tag{3}$$

where $f(\theta)$ is an unknown function to be determined, and R_0 is a given positive constant, such that the disk $D = \{(r,\theta)|r \le R_0,\ 0 \le \theta \le 2\pi\}$ can cover Ω for the interior problem, or it is inside in the complement of Ω, that is, $D \in \Omega^c$ for the exterior problem. Fig. 1 schematically shows a relation between R_0 and ρ for the interior problem.

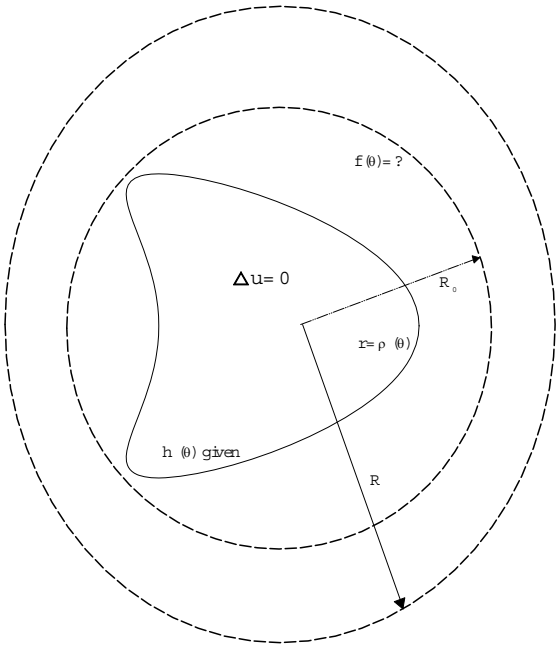

Figure 1: Schematically displaying the domain for the interior problem and the relations of R_0 and R with respect to the boundary.

Specifically, we can let

$$R_0 \le \rho_{\min} = \min_{\theta\in[0,2\pi]} \rho(\theta) \ \ \text{(exterior problem)}, \tag{4}$$

$$R_0 \ge \rho_{\max} = \max_{\theta\in[0,2\pi]} \rho(\theta) \ \ \text{(interior problem)}. \tag{5}$$

Thus, we have a Fourier series expansion for $u(r,\theta)$ satisfying Eqs. (1) and (3):

$$u(r,\theta) = a_0 + \sum_{k=1}^{\infty} \left[a_k \left(\frac{R_0}{r}\right)^{\pm k} \cos k\theta + b_k \left(\frac{R_0}{r}\right)^{\pm k} \sin k\theta \right], \tag{6}$$

where

$$a_0 = \frac{1}{2\pi}\int_0^{2\pi} f(\xi)d\xi, \tag{7}$$

$$a_k = \frac{1}{\pi}\int_0^{2\pi} f(\xi)\cos k\xi d\xi, \tag{8}$$

$$b_k = \frac{1}{\pi}\int_0^{2\pi} f(\xi)\sin k\xi d\xi. \tag{9}$$

In Eq. (6) the positive sign before k is used for the exterior problem, while the minus sign before k is used for the interior problem.

By imposing the condition (2) on Eq. (6) we obtain

$$a_0 + \sum_{k=1}^{\infty} B^k(\theta)[a_k \cos k\theta + b_k \sin k\theta] = h(\theta), \tag{10}$$

where

$$B(\theta) := \left(\frac{R_0}{\rho(\theta)}\right)^{\pm 1}, \tag{11}$$

in which +1 is for exterior problem, and -1 is for interior problem.

It is known that for the Laplace equation in the two-dimensional domain the set

$$\left\{1, r^{\mp k}\cos k\theta, r^{\mp k}\sin k\theta, \ k = 1,2,\ldots\right\} \tag{12}$$

forms the T-complete functions, and the solution can be expanded by these bases [Kita and Kamiya (1995); Li, Lu, Huang and Cheng (2006)]:

$$u(r,\theta) = \overline{a}_0 + \sum_{k=1}^{\infty} [\overline{a}_k r^{\mp k}\cos k\theta + \overline{b}_k r^{\mp k}\sin k\theta]. \tag{13}$$

It is simply a direct consequence of Eq. (6) by inserting $R_0 = 1$.

In Sections 5 and 6, we will address the ill-conditioning problem of the Trefftz method, where one can see that the present method will lead to a big improvement of the ill-conditioning problem [Liu (2007d,2008)].

3 The collocation method

The series expansion in Eq. (10) is well suited in the range of $\theta \in [0,2\pi]$. Hence, we may have an admissible function with finite terms

$$a_0 + \sum_{k=1}^{m} B^k(\theta)[a_k \cos k\theta + b_k \sin k\theta] = h(\theta), \quad 0 \le \theta \le 2\pi. \tag{14}$$

Our next task is to find $a_k, b_k, \ k = 0,1,\ldots,m$ from Eq. (14).

Eq. (14) is imposed at $n = 2m+1$ different collocated points θ_i on the interval of $0 \le \theta_i \le 2\pi$:

$$a_0 + \sum_{k=1}^{m} B^k(\theta_i)[a_k \cos k\theta_i + b_k \sin k\theta_i] = h(\theta_i). \tag{15}$$

Let

$$\theta_i = i\Delta\theta, \quad i = 1, \ldots, n, \tag{16}$$

where $\Delta\theta = 2\pi/n$. When the index i in Eq. (15) runs from 1 to n we obtain a linear equations system with dimensions $n = 2m+1$:

$$\begin{bmatrix} 1 & B(\theta_1)\cos\theta_1 & B(\theta_1)\sin\theta_1 & \ldots \\ 1 & B(\theta_2)\cos\theta_2 & B(\theta_2)\sin\theta_2 & \ldots \\ \vdots & \vdots & \vdots & \vdots \\ 1 & B(\theta_{n-1})\cos\theta_{n-1} & B(\theta_{n-1})\sin\theta_{n-1} & \ldots \\ 1 & B(\theta_n)\cos\theta_n & B(\theta_n)\sin\theta_n & \ldots \end{bmatrix}$$
$$\begin{bmatrix} B^m(\theta_1)\cos(m\theta_1) & B^m(\theta_1)\sin(m\theta_1) \\ B^m(\theta_2)\cos(m\theta_2) & B^m(\theta_2)\sin(m\theta_2) \\ \vdots & \vdots \\ B^m(\theta_{n-1})\cos(m\theta_{n-1}) & B^m(\theta_{n-1})\sin(m\theta_{n-1}) \\ B^m(\theta_n)\cos(m\theta_n) & B^m(\theta_n)\sin(m\theta_n) \end{bmatrix}$$
$$\begin{bmatrix} a_0 \\ a_1 \\ b_1 \\ \vdots \\ a_m \\ b_m \end{bmatrix} = \begin{bmatrix} h(\theta_1) \\ h(\theta_2) \\ \vdots \\ h(\theta_{n-1}) \\ h(\theta_n) \end{bmatrix}. \tag{17}$$

We denote the above equation by

$$\mathbf{Rx} = \mathbf{h}, \tag{18}$$

where

$$\mathbf{x} = (a_0, a_1, b_1, \cdots, a_m, b_m)^{\mathrm{T}} \tag{19}$$

is the vector of unknown coefficients. The superscript T signifies the transpose.

The conjugate gradient method can be used to solve the following normal equation:

$$\mathbf{Ax} = \mathbf{b}, \tag{20}$$

where

$$\mathbf{A} := \mathbf{R}^{\mathrm{T}}\mathbf{R}, \quad \mathbf{b} := \mathbf{R}^{\mathrm{T}}\mathbf{h}. \tag{21}$$

Inserting the calculated $\mathbf{x}$ into Eq. (6) we can calculate $u(r,\theta)$ at any point in the problem domain by

$$u(r,\theta) = x_1 + \sum_{k=1}^{m} \left[x_{2k} \left(\frac{R_0}{r}\right)^{\pm k} \cos k\theta + x_{2k+1} \left(\frac{R_0}{r}\right)^{\pm k} \sin k\theta \right]. \tag{22}$$

4 The method of fundamental solutions

In the potential theory, it is well known that the method of fundamental solutions (MFS) can be used to solve the Laplace problems when a fundamental solution is known.

In the MFS the solution of u at the field point $x = (r\cos\theta, r\sin\theta)$ can be expressed as a linear combination of fundamental solutions $U(x, s_j)$:

$$u(x) = \sum_{j=1}^{n} c_j U(x, s_j), \quad s_j \in \Omega^c, \tag{23}$$

where n is the number of source points, c_j are the unknown coefficients, and s_j are the source points. For the Laplace equation we have the fundamental solutions

$$U(x, s_j) = \ln r_j, \quad r_j = |x - s_j|. \tag{24}$$

In the practical application of MFS, usually the source points are uniformly located on a circle with a radius R as shown in Fig. 1, such that after imposing the boundary condition (2) on Eq. (23) we obtain a linear equations system:

$$\mathbf{Uz} = \mathbf{h}, \tag{25}$$

where $x_i = (\rho(\theta_i)\cos\theta_i, \rho(\theta_i)\sin\theta_i)$, $s_j = (R\cos\theta_j, R\sin\theta_j)$, and

$$\begin{aligned} U_{ij} &= U(x_i, s_j), \\ \mathbf{z} &= (c_1, \cdots, c_n)^{\mathrm{T}}, \\ \mathbf{h} &= (h(\theta_1), \cdots, h(\theta_n))^{\mathrm{T}}. \end{aligned} \tag{26}$$

Then, the conjugate gradient method can be employed to solve the normal form of Eq. (25) to determine the coefficients c_j.

The above process to find the coefficients is amount to solve a linear square problem, of which a detailed description was given by Golberg and Chen (1996).

5 The ill-conditioning of linear systems

In order to demonstrate our analysis of the ill-conditioning problem of both the F- and T-Trefftz methods, we first limit ourself to a simpler interior problem with the boundary to be a circle with a radius a. Then, in Section 6 we will return to the Laplace interior problem with arbitrary plane domain.

It is known that the fundamental solution for Laplace equation in a plane domain can be expressed by [Chen, Wu, Lee and Chen (2007)]

$$U(x,s) = \ln R - \sum_{k=1}^{\infty} \frac{1}{k} \left(\frac{r}{R}\right)^k \cos k(\theta - \phi), \tag{27}$$

where $x = (r,\theta)$ and $s = (R,\phi)$ are the polar coordinates of x and s. Therefore, Eq. (23) can be expressed as

$$u(r,\theta) = \sum_{j=1}^{n} c_j \left[\ln R - \sum_{k=1}^{\infty} \frac{1}{k} \left(\frac{r}{R}\right)^k \cos k(\theta - \theta_j) \right]. \tag{28}$$

Along the above mentioned circle we have

$$u(a,\theta) = \sum_{j=1}^{n} c_j \left[\ln R - \sum_{k=1}^{\infty} \frac{1}{k} \left(\frac{a}{R}\right)^k \cos k(\theta - \theta_j) \right]. \tag{29}$$

On the other hand, from Eq. (13) we obtain the Trefftz representation of $u(a,\theta)$ as follows:

$$u(a,\theta) = \overline{a}_0 + \sum_{k=1}^{m} [\overline{a}_k a^k \cos k\theta + \overline{b}_k a^k \sin k\theta]. \tag{30}$$

Upon taking $2m+1 = n$, truncating the higher modes than m in Eq. (29), and equating the above two equations, we obtain

$$\overline{a}_0 = \sum_{j=1}^{n} c_j \ln R, \tag{31}$$

$$\overline{a}_k = -\sum_{j=1}^{n} c_j \frac{1}{kR^k} \cos(k\theta_j), \tag{32}$$

$$\overline{b}_k = -\sum_{j=1}^{n} c_j \frac{1}{kR^k} \sin(k\theta_j). \tag{33}$$

Upon letting

$$\mathbf{y} = (\overline{a}_0, \overline{a}_1, \overline{b}_1, \cdots, \overline{a}_m, \overline{b}_m)^{\mathrm{T}}, \tag{34}$$

$$\mathbf{z} = (c_1, \cdots, c_n)^{\mathrm{T}}, \tag{35}$$

from Eqs. (31)-(33) follows a linear relation between $\mathbf{y}$ and $\mathbf{z}$:

$$\mathbf{y} = \mathbf{K}_1 \mathbf{z}, \tag{36}$$

where

$$\mathbf{K}_1 = \begin{bmatrix} \ln R & \ln R \\ -\frac{1}{R}\cos\theta_1 & -\frac{1}{R}\cos\theta_2 \\ -\frac{1}{R}\sin\theta_1 & -\frac{1}{R}\sin\theta_2 \\ \vdots & \vdots \\ -\frac{1}{mR^m}\cos(m\theta_1) & -\frac{1}{mR^m}\cos(m\theta_2) \\ -\frac{1}{mR^m}\sin(m\theta_1) & -\frac{1}{mR^m}\sin(m\theta_2) \end{bmatrix} \begin{bmatrix} \ln R & \cdots & \ln R \\ -\frac{1}{R}\cos\theta_3 & \cdots & -\frac{1}{R}\cos\theta_n \\ -\frac{1}{R}\sin\theta_3 & \cdots & -\frac{1}{R}\sin\theta_n \\ \vdots & \cdots & \vdots \\ -\frac{1}{mR^m}\cos(m\theta_3) & \cdots & -\frac{1}{mR^m}\cos(m\theta_n) \\ -\frac{1}{mR^m}\sin(m\theta_3) & \cdots & -\frac{1}{mR^m}\sin(m\theta_n) \end{bmatrix}. \tag{37}$$

Eq. (36) describes a relation between the Trefftz method and the MFS first derived by Chen, Wu, Lee and Chen (2007).

However, the matrix $\mathbf{K}_1$ is ill-conditioned as shown in Fig. 2, where we have fixed $m = 17$ and let R run in the interval $[1.1, 3]$. The condition number used here is defined by

$$\mathrm{Cond}(\mathbf{K}_1) = \|\mathbf{K}_1\| \|\mathbf{K}_1^{-1}\|. \tag{38}$$

The norm for $\mathbf{K}_1$ is the Frobenius norm. For more large m and R the ill-condition of $\mathbf{K}_1$ is increased fast as reflected by its condition number.

Now we turn to the relation between the MFS and the modified Trefftz method (MTM). For the interior problem we compare Eqs. (6) and (13) by taking the minus sign for the former and the positive sign for the latter. Thus we have

$$a_0 = \overline{a}_0, \quad a_k = R_0^k \overline{a}_k, \quad b_k = R_0^k \overline{b}_k, \tag{39}$$

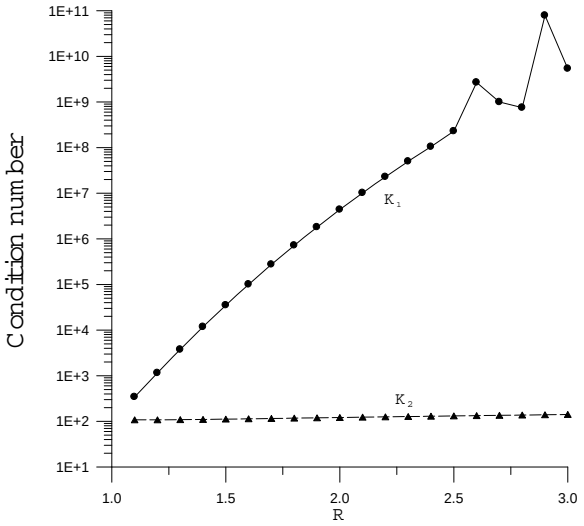

Figure 2: Comparing the condition numbers of $\mathbf{K}_1$ and $\mathbf{K}_2$ for different R.

and come to the following relation by taking $R_0 = R$:

$$\mathbf{x} = \mathbf{K}_2 \mathbf{z}, \tag{40}$$

where

$$\mathbf{K}_2 = \begin{bmatrix} \ln R & \ln R \\ -\cos\theta_1 & -\cos\theta_2 \\ -\sin\theta_1 & -\sin\theta_2 \\ \vdots & \vdots \\ -\frac{1}{m}\cos(m\theta_1) & -\frac{1}{m}\cos(m\theta_2) \\ -\frac{1}{m}\sin(m\theta_1) & -\frac{1}{m}\sin(m\theta_2) \end{bmatrix} \begin{bmatrix} \ln R & \cdots & \ln R \\ -\cos\theta_3 & \cdots & -\cos\theta_n \\ -\sin\theta_3 & \cdots & -\sin\theta_n \\ \vdots & \cdots & \vdots \\ -\frac{1}{m}\cos(m\theta_3) & \cdots & -\frac{1}{m}\cos(m\theta_n) \\ -\frac{1}{m}\sin(m\theta_3) & \cdots & -\frac{1}{m}\sin(m\theta_n) \end{bmatrix}. \tag{41}$$

Similarly, we plot the condition number of $\mathbf{K}_2$ in Fig. 2 for a comparison with $\mathbf{K}_1$. It can be seen that the condition number of $\mathbf{K}_2$ is insensitive to R, and when R increases, the condition number of $\mathbf{K}_2$ is much smaller than that of $\mathbf{K}_1$. Contrasting to $\mathbf{K}_1$, $\mathbf{K}_2$ is always well-conditioned even for more large m and R.

The above discussions indicate that when one obtains the coefficients $\mathbf{y}$ by the Trefftz method, it is hard to precisely obtain the coefficients $\mathbf{z}$ of the MFS from Eq. (36) because $\mathbf{K}_1$ is ill-conditioned. Conversely, when one obtains the coefficients $\mathbf{x}$ by the modified Trefftz method, it can precisely obtain the coefficients $\mathbf{z}$ of the MFS from Eq. (40) because $\mathbf{K}_2$ is well-conditioned.

Indeed, we will use the above mentioned circle to verify that both the linear systems resulting from the TM and the MFS are ill-conditioned. Conversely, the linear system resulting from the MTM is well-conditioned. In order to show this fact we display the condition numbers for the resulting linear systems of these three methods in Fig. 3(a), where $a = 2$ was fixed, and for the TM one uses $R_0 = 1$, for the MTM one uses $R_0 = 2$, and for the MFS one uses $R = 4$. It can be seen that the condition numbers for the TM and the MFS are much larger than that of the MTM. Under these situations we may expect that the numerical solution provided by the MTM may be accurate than those provided by the TM and the MFS. For definite we consider an exact solution $u = x^2 - y^2 = r^2\cos(2\theta)$ along a circle with a radius $r = 1$. Under the following parameters $m = 15$ and $n = 31$, the numerical errors are plotted in Fig. 3(b), where for the TM one uses $R_0 = 1$, for the MTM one uses $R_0 = 2$, and for the MFS one uses $R = 8$. It can be seen that the numerical errors for the TM is much larger than that of the MFS and the MTM. The MFS is accurate than the TM, but it is still less accurate than the MTM about three orders. The numerical accuracy provided by the MTM is almost within the machinery accuracy.

6 Mitigating the ill-conditioning of MFS

Mathematically speaking, the MFS can be made more accurate, if one can mitigate its ill-conditioning of the linear equations system in Eq. (25). However, there has no such result in the open literature of MFS.

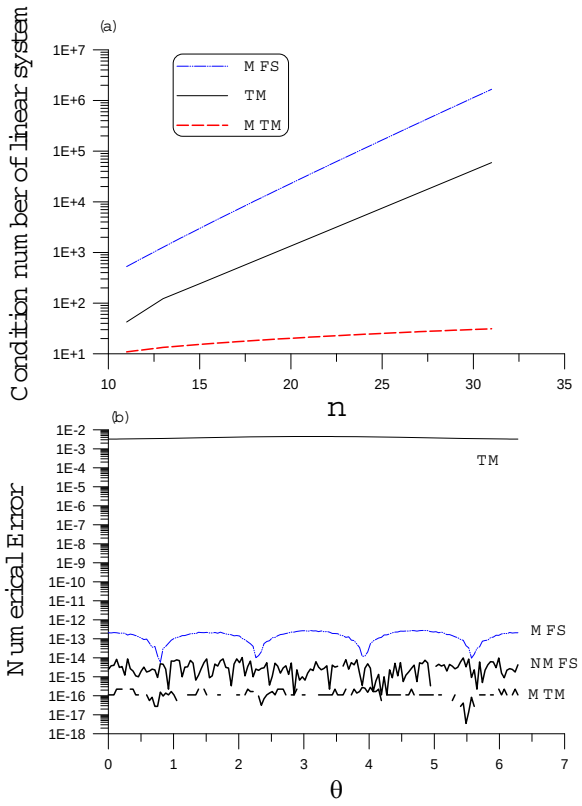

Figure 3: Considering an exact solution $u = x^2 - y^2$ with a circular boundary with radius 2, (a) comparing the condition numbers of TM, MFS and MTM, and (b) comparing the numerical errors by the TM, MFS, NMFS and MTM.

6.1 Normalized fundamental solutions

About the MFS, Cheng (1987) has studied the Dirichlet boundary condition where the interior domain is a circle of radius a and the source points are located uniformly around a disk of radius $R > a$. The collocated points are also uniformly spaced around the boundary to match the boundary condition. In this case he has shown that the error of the numerical solution u_n is governed by

$$\max_{\Omega} |u - u_n| \le c \left(\frac{a}{R} \right)^n, \tag{42}$$

where c is a constant. Hence, it can be seen that the error decreases exponentially with respect to n and R. For the purpose of numerical calculations it is better to use a moderate n but tries to take R as large as possible. Unfortunately, the condition number of MFS increases like as e^R as shown in Fig. 4(a) by the heavy dashed line, where we are fixed $a = 2$ and $n = 20$ and let R change in the interval of $a < R \le 10$.

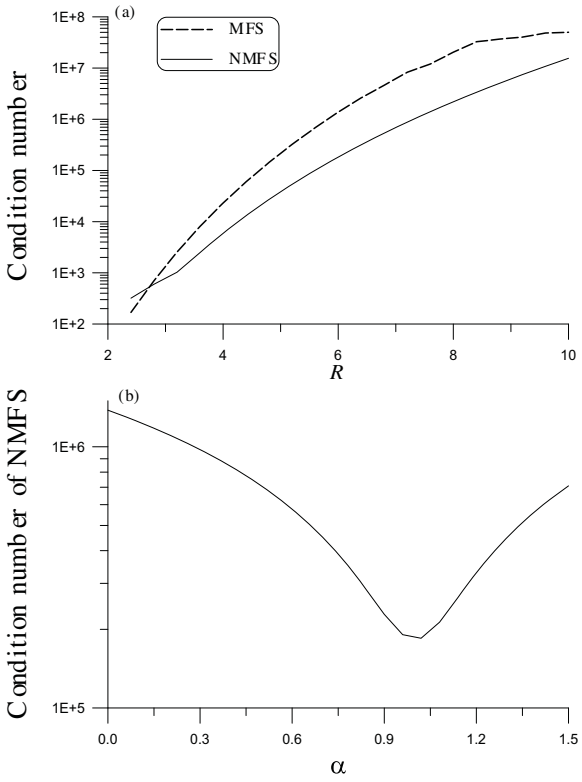

Figure 4: (a) Comparing the condition numbers of MFS and NMFS, and (b) plotting the condition number of NMFS with respect to α.

Inspired by the works of Han and Olson (1987) and Smyrlis and Karageorghis (2001, 2003), one may use the following expansion:

$$u(x) = \sum_{j=1}^{n} c_j \overline{U}(x, s_j), \quad s_j \in \Omega^c, \tag{43}$$

$$\overline{U}(x, s_j) = \ln \frac{r_j}{R^\alpha}, \quad r_j = |x - s_j|. \tag{44}$$

When $\alpha = 0$ we can recover to the original MFS. In Fig. 4(a) we use the solid line to express its improvement of reducing the condition number, where we are fixed $a = 2$, $n = 20$, $\alpha = 1.001$ and let R change in the interval of $a < R \le 10$. When $R = 10$, the condition number of MFS is about

2.3×10^9, which is reduced to about 3×10^7 for the normalized MFS (NMFS). In Fig. 4(b) we plot the variation of condition number with respect to α, but fixed $R=6$ and $n=20$. It can be seen that near $\alpha=1$ there exists a minimum. For the numerical example in Fig. 3, we also compare the numerical error of the NMFS with other methods, where $R=8$, $n=31$ and $\alpha=1$ were used. Upon comparing with the MFS, the NMFS can increase the accuracy about two orders. However, this improvement is limited.

6.2 A significant improvement of MFS

Encouraged by a big improvement of the new modification of the Trefftz method, we may attempt to directly correlate Eqs. (18) and (25). For this purpose we require to construct a relation as that Eq. (40) for the circular boundary.

Suppose that Eq. (28) is imposed on the boundary by

$$u(\rho(\theta),\theta)= \sum_{j=1}^{n} c_j\left[\ln R-\sum_{k=1}^{\infty}\frac{1}{k}\left(\frac{\rho}{R}\right)^k\cos k(\theta-\theta_j)\right]. \quad (45)$$

On the other hand, from Eq. (6) we obtain a corresponding modified Trefftz equation on the boundary:

$$u(\rho(\theta),\theta)= a_0+\sum_{k=1}^{\infty}\left[a_k\left(\frac{\rho}{R_0}\right)^k\cos k\theta+b_k\left(\frac{\rho}{R_0}\right)^k\sin k\theta\right]. \quad (46)$$

Upon taking $2m+1=n$, truncating the higher modes than m in Eqs. (45) and (46), and equating the above two equations, we obtain the following sufficient conditions:

$$a_0=\sum_{j=1}^{n}c_j\ln R, \quad (47)$$

$$a_k=-\sum_{j=1}^{n}c_j\frac{R_0^k}{kR^k}\cos(k\theta_j), \quad (48)$$

$$b_k=-\sum_{j=1}^{n}c_j\frac{R_0^k}{kR^k}\sin(k\theta_j). \quad (49)$$

Defining $\mathbf{x}$ as that in Eq. (19) and $\mathbf{z}$ as that in Eq. (36), from Eqs. (47)-(49) it follows a definite relation between $\mathbf{x}$ and $\mathbf{z}$:

$$\mathbf{x}=\mathbf{K}\mathbf{z}, \quad (50)$$

where

$$\mathbf{K}=\begin{bmatrix} \ln R & \ln R & \cdots & \ln R \\ -\frac{R_0}{R}\cos\theta_1 & -\frac{R_0}{R}\cos\theta_2 & \cdots & -\frac{R_0}{R}\cos\theta_n \\ -\frac{R_0}{R}\sin\theta_1 & -\frac{R_0}{R}\sin\theta_2 & \cdots & -\frac{R_0}{R}\sin\theta_n \\ \vdots & \vdots & \cdots & \vdots \\ -\frac{R_0^m}{mR^m}\cos(m\theta_1) & -\frac{R_0^m}{mR^m}\cos(m\theta_2) & \cdots & -\frac{R_0^m}{mR^m}\cos(m\theta_n) \\ -\frac{R_0^m}{mR^m}\sin(m\theta_1) & -\frac{R_0^m}{mR^m}\sin(m\theta_2) & \cdots & -\frac{R_0^m}{mR^m}\sin(m\theta_n) \end{bmatrix}. \quad (51)$$

It should be stressed that the relation (50) is independent of the boundary shape, and when $R_0=R$ the matrix $\mathbf{K}$ is reduced to $\mathbf{K}_2$.

We need to mention that in the paper by Chen, Wu, Lee and Chen (2007) the relation of Trefftz method and the MFS has been set up for a unit circle, which means that $R_0=1$ in Eq. (51). Now, we extend this relation to arbitrary domain with a characteristic length R_0 determined by the physical problem.

Now, utilizing Eqs. (18) and (50) we obtain a very important formulation:

$$\mathbf{U}_m\mathbf{z}=\mathbf{h}, \quad (52)$$

$$\mathbf{U}_m:=\mathbf{R}\mathbf{K}, \quad (53)$$

where

$$\mathbf{R}=$$

$$\begin{bmatrix} 1 & B(\theta_1)\cos\theta_1 & B(\theta_1)\sin\theta_1 & \dots \\ 1 & B(\theta_2)\cos\theta_2 & B(\theta_2)\sin\theta_2 & \dots \\ \vdots & \vdots & \vdots & \vdots \\ 1 & B(\theta_{n-1})\cos\theta_{n-1} & B(\theta_{n-1})\sin\theta_{n-1} & \dots \\ 1 & B(\theta_n)\cos\theta_n & B(\theta_n)\sin\theta_n & \dots \end{bmatrix}$$
$$\begin{bmatrix} B^m(\theta_1)\cos(m\theta_1) & B^m(\theta_1)\sin(m\theta_1) \\ B^m(\theta_2)\cos(m\theta_2) & B^m(\theta_2)\sin(m\theta_2) \\ \vdots & \vdots \\ B^m(\theta_{n-1})\cos(m\theta_{n-1}) & B^m(\theta_{n-1})\sin(m\theta_{n-1}) \\ B^m(\theta_n)\cos(m\theta_n) & B^m(\theta_n)\sin(m\theta_n) \end{bmatrix} \tag{54}$$

The boundary shape influences the solution of $\mathbf{z}$ through the term $B = \rho(\theta)/R_0$ appeared in the matrix $\mathbf{R}$. Upon comparing with Eq. (25), we call the present $\mathbf{U}_m$ a modification of $\mathbf{U}$. Although $\mathbf{U}$ is ill-conditioning, the new $\mathbf{U}_m$ will be proved to be well-conditioning by the following numerical examples. In the present formulation, the R-circle is no more required to be far from the boundary as suggested in the literature of MFS, and in practice we can take $R = R_0$ for simplicity. We should stress that the present modification is not of the preconditioning type for the MFS, because Eq. (52) cannot be obtained from Eq. (25) by simply multiplying a preconditioning matrix on both the sides.

We find that $\mathbf{K}$ can be decomposed as

$$\mathbf{K} = \mathbf{T}_R \mathbf{T}_\theta, \tag{55}$$

where

$$\mathbf{T}_R = \begin{bmatrix} \ln R & 0 & 0 & 0 & \cdots & 0 & 0 \\ 0 & -\frac{R_0}{R} & 0 & 0 & \cdots & 0 & 0 \\ 0 & 0 & -\frac{R_0}{R} & 0 & \cdots & 0 & 0 \\ \vdots & \vdots & \vdots & \dots & \vdots & \vdots & \vdots \\ 0 & 0 & 0 & 0 & \cdots & -\frac{R_0^m}{mR^m} & 0 \\ 0 & 0 & 0 & 0 & \cdots & 0 & -\frac{R_0^m}{mR^m} \end{bmatrix}, \tag{56}$$

$$\mathbf{T}_\theta = \begin{bmatrix} 1 & 1 & 1 & \cdots & 1 \\ \cos\theta_1 & \cos\theta_2 & \cos\theta_3 & \cdots & \cos\theta_n \\ \sin\theta_1 & \sin\theta_2 & \sin\theta_3 & \cdots & \sin\theta_n \\ \vdots & \vdots & \vdots & \cdots & \vdots \\ \cos(m\theta_1) & \cos(m\theta_2) & \cos(m\theta_3) & \cdots & \cos(m\theta_n) \\ \sin(m\theta_1) & \sin(m\theta_2) & \sin(m\theta_3) & \cdots & \sin(m\theta_n) \end{bmatrix}. \tag{57}$$

Furthermore, due to the orthogonal property of $\mathbf{T}_\theta$

$$\mathbf{T}_\theta \mathbf{T}_\theta^T = \begin{bmatrix} n & 0 & 0 & \cdots & 0 \\ 0 & \frac{n}{2} & 0 & \cdots & 0 \\ 0 & 0 & \frac{n}{2} & \cdots & 0 \\ \vdots & \vdots & \vdots & \dots & \vdots \\ 0 & 0 & 0 & \cdots & \frac{n}{2} \end{bmatrix}, \tag{58}$$

we can prove that

$$\det(\mathbf{T}_\theta) = \frac{n^{m+\frac{1}{2}}}{2^m}. \tag{59}$$

Therefore, we can prove that $\mathbf{K}$ is invertible (see Appendix A), and in view of Eq. (56) by inserting $R = R_0$, $\mathbf{K}$ is also well-conditioned, such that in the calculation of $\mathbf{z}$ by Eq. (52) we suggest to use

$$\mathbf{z} = \mathbf{K}^{-1}(\mathbf{R}^T\mathbf{R})^{-1}\mathbf{R}^T\mathbf{h}. \tag{60}$$

In Appendix A we have derived an explicit form of $\mathbf{K}^{-1}$. After $\mathbf{z}$ is solving from the above equation, we can insert it into Eq. (23) to calculate the solution of u.

In order to distinct these two methods in this section from the method of fundamental solutions (MFS) in Section 4, we will call the method in Section 6.1 the normalized MFS (NMFS), while the method in Section 6.2 the modified MFS (MMFS). Also for the shorthand of notations we will use TM to denote the Trefftz method and the MTM to denote the modified Trefftz method.

7 Numerical examples

In this section we will apply the new method of MMFS on interior problems.

7.1 Example 1 (interior problem)

In this example we consider a complex epitrochoid boundary shape

$$\rho(\theta)=\sqrt{(a+b)^2+1-2(a+b)\cos(a\theta/b)}, \tag{61}$$

$$x(\theta)=\rho\cos\theta,\quad y(\theta)=\rho\sin\theta \tag{62}$$

with $a=4$ and $b=1$. For the purpose of comparison we also consider an exact solution:

$$u(x,y)=x^2-y^2. \tag{63}$$

The exact boundary data can be obtained by inserting Eqs. (61) and (62) into the above equation.

Before computing this example we use it to demonstrate the improvement by using the MMFS. In Fig. 5 we compare the condition numbers of the linear systems resulting from the use of MFS, NMFS and MMFS on this example, from which it can be seen that the MMFS has the smallest condition number than the other two methods. When the condition numbers of MFS and NMFS increase fast with respect to n, the condition number of MMFS increases slowly.

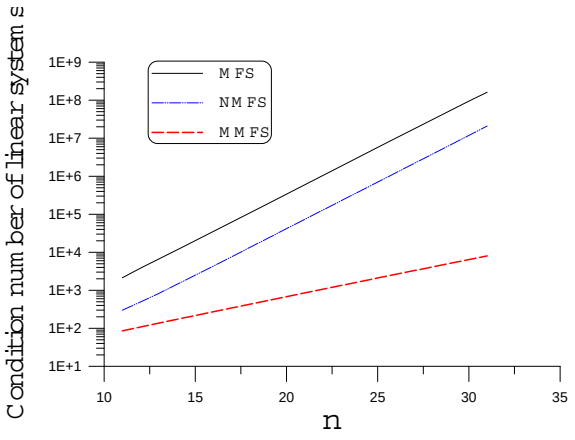

Figure 5: For Example 1 we comparing the condition numbers of MFS, NMFS and MMFS with different n.

The contour shape of this example is plotted in the inset of Fig. 6. In the numerical computations we have fixed $R=R_0=6$ and $m=25$ for the MTM and MMFS. In Fig. 6(a) we compare the numerical solutions with the exact solution along a circle with radius $r=3$, while the numerical errors are plotted in Fig. 6(b) with the heavy-dashed line for the MTM and the solid line for the MMFS. When we apply the MFS to this example we adjust the best parameters with $R=20$ and $n=30$, whose error is plotted in Fig. 6(b) with the dashed line. For the NMFS we use $R=25$, $n=40$ and $\alpha=1$, whose error is plotted in Fig. 6(b) with the dashed-dotted line. The accuracy of the MMFS is better than the NMFS and then than the MFS, and is competitive with the MTM. For all these methods very accurate numerical solutions are obtained with absolute errors smaller than 10^{-8}. This example reveals the improvements over the MFS by using the NMFS about three orders and further by using the MMFS about five orders.

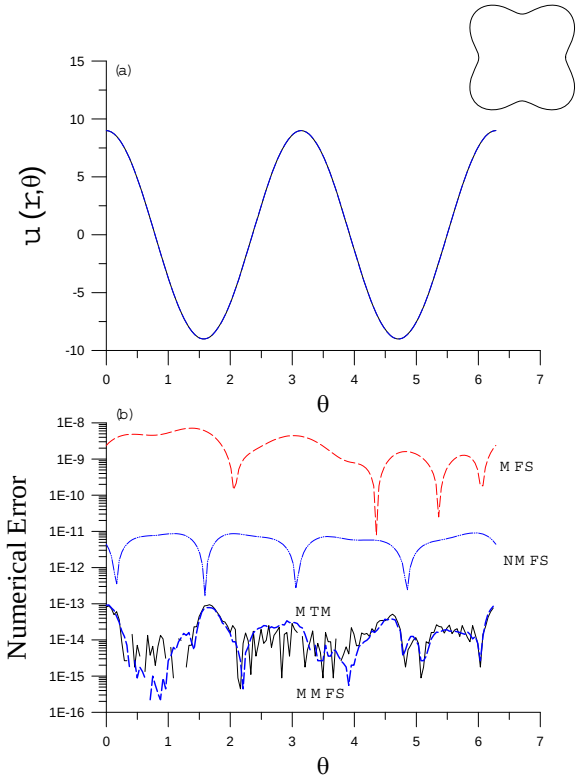

Figure 6: For Example 1, (a) comparing the numerical solutions with exact solution, and (b) comparing the numerical errors by the MFS, NMFS, MMFS and MTM.

7.2 Example 2 (interior problem)

In this example we consider the same epitrochoid boundary shape as given by Eqs. (61) and (62) with $a = 4$ and $b = 1$, but with a more complex solution given by

$$u(x,y) = e^x \cos y. \tag{64}$$

In the numerical computations we have fixed $R = R_0 = 6$ and $m = 25$ for the MTM and MMFS. In Fig. 7(a) we compare the numerical solutions with the exact solution along a circle with radius $r = 3$, while the numerical errors are plotted in Fig. 7(b) with the solid line for the MTM and the heavy-dashed-line for the MMFS. When we apply the MFS to this example we adjust the best parameters with $R = 7$ and $n = 120$, whose error is plotted in Fig. 7(b) with the dashed line. For the NMFS we use $R = 7$, $n = 150$ and $\alpha = 1.1$, whose error is plotted in Fig. 7(b) with the dashed-dotted line. The accuracy of the MTM and MMFS is much better than the NMFS and then than the MFS. This example shows again a big improvement over the MFS and NMFS by using the MMFS.

7.3 Example 3 (interior problem)

In this example we consider the exact solution given by Eq. (64) again, but with the following boundary:

$$\rho(\theta) = \sqrt{\cos(2\theta) + \sqrt{2 - \sin^2(2\theta)}}. \tag{65}$$

This example has been computed by Ramachandran (2002) and Chen, Cho and Golberg (2006) through the MFS together with the singular value decomposition (SVD) and the Gaussian elimination methods to solve the resulting linear system. As they are, we place 40 collocation and source points on the boundary and the artificial circle with a source radius $R = R_0$. In Table 1 we compare the absolute maximum errors along the boundary calculated by the MTM and the MMFS with the results provided by Chen, Cho and Golberg (2006). Under moderate radius, the present solutions with $R = 2, 3, 5$ are better than that calculated by Chen, Cho and Golberg (2006).

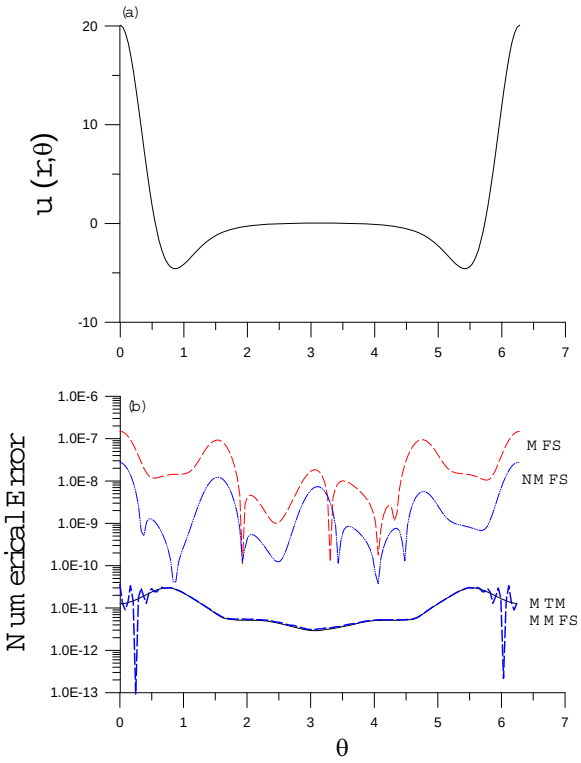

Figure 7: For Example 2, (a) comparing the numerical solutions with exact solution, and (b) comparing the numerical errors by the MFS, NMFS, MMFS and MTM.

Table 1: For Example 3 we comparing the maximum errors of the present methods with those in Chen, Cho and Golberg (2006) under different source radius

R	SVD	MTM	MMFS
2	2.00×10^{-4}	2.55×10^{-9}	3.32×10^{-5}
3	1.17×10^{-9}	5.57×10^{-12}	1.08×10^{-10}
5	7.54×10^{-10}	2.70×10^{-11}	2.71×10^{-11}
8	2.26×10^{-9}	1.85×10^{-8}	1.85×10^{-8}
10	4.45×10^{-10}	2.09×10^{-7}	2.09×10^{-7}
20	1.02×10^{-7}	2.24×10^{-7}	2.47×10^{-7}

In order to compare the present results with that calculated by Ramachandran (2002), we define the L^2 error by

$$\text{Error}(u_{L^2}) = \sum_{i=1}^{N} |u(i) - u_n(i)|^2, \tag{66}$$

where u and u_n denotes the exact and numerical solution, respectively, and N is the total number of

calculated points on the boundary. In Table 2 we compare the Error(u_{L^2}) calculated by the MTM and the MMFS with the results from Ramachandran (2002). It can be seen that our results are much better than that calculated by Ramachandran (2002).

Table 2: For Example 3 we comparing the L^2 errors of the present methods with those in Ramachandran (2002) under different source radius

R	SVD	MTM	MMFS
1.75	7.81×10^{-5}	2.14×10^{-14}	3.10×10^{-5}
2	9.79×10^{-9}	4.10×10^{-17}	2.39×10^{-9}
3	1.42×10^{-9}	1.41×10^{-22}	2.65×10^{-20}
5	3.99×10^{-7}	1.64×10^{-20}	1.64×10^{-20}
10	2.42×10^{-2}	1.37×10^{-12}	1.37×10^{-12}
20	4.56×10^{-1}	1.56×10^{-12}	1.63×10^{-12}

7.4 Example 4 (exterior problem)

In this example we consider a complex epitrochoid boundary shape given by Eqs. (61) and (62) with $a=3$ and $b=1$. The analytical solution is given by

$$u(x,y)=\exp\left(\frac{x}{x^2+y^2}\right)\cos\left(\frac{y}{x^2+y^2}\right). \qquad (67)$$

The exact boundary data can be easily derived by inserting Eqs. (61) and (62) into the above equation.

We have applied the MTM to this example by using $R_0=2$ and $m=50$. In Fig. 8(a) we compare the exact solution with numerical solution along a circle with radius 10. It can be seen that the numerical solution is almost coincident with the exact solution. The numerical error is plotted in Fig. 8(b) with the solid line, of which we can see that the new method has absolute error smaller than 10^{-10}. The MFS cannot be applied to this problem. For the NMFS we use $R=2.99$, $n=20$ and $\alpha=-500$, whose error is plotted in Fig. 8(b) with the dashed line. The accuracy of the MTM is much better than the NMFS.

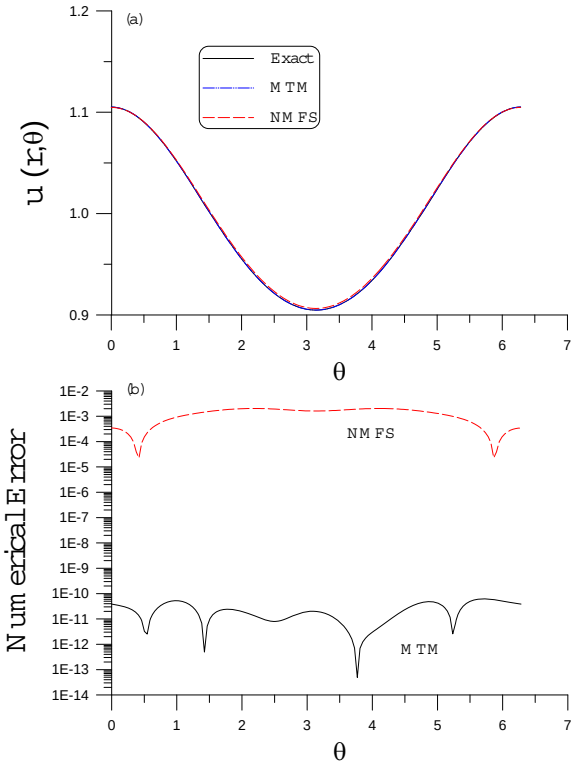

Figure 8: For Example 4, (a) comparing the numerical solutions with exact solution, and (b) comparing the numerical errors by the NMFS and MTM.

8 Conclusions

In this paper we have proposed a new method to modify the MFS to calculate the solutions of Laplace problems in arbitrary plane domains. In practice, the MTM is a modified Trefftz method by taking the domain's characteristic length R_0 into account. With the aid of MTM, we have constructed an exact relation between the MFS and MTM, which brings out a new linear equations system (60) to solve the unknown coefficients $\mathbf{z}$ for the MMFS. In doing so, we can largely alleviate the ill-conditioning of MFS, and as a byproduct we can raise the accuracy over four orders more than the original MFS. Numerical examples indicate that both the MTM and MMFS can attain highly accurate numerical solutions with the accuracy about in the orders from 10^{-10} to 10^{-18}. For the MFS there is still a problem to suitably choose the source radius. When it is theoreti-

cally proved that larger source radius results in worse condition number and better accuracy, how to making a trade-off between these two tendencies is still a problem. Conversely, for the MMFS we can take $R = R_0$ to be the maximum radius of the boundary, and there is no problem to choose the source radius. The basic idea employed here may be extended to other type elliptic problems. However, this will be a main issue of our forthcoming works.

Acknowledgement: Taiwan's National Science Council project NSC-96-2221-E-019-027-MY3 granted to the author is highly appreciated.

Appendix A

In this appendix we derive the inverse of $\mathbf{K}$. First we note that $\mathbf{T}_\theta$ can be decomposed as

$$\mathbf{T}_\theta = \begin{bmatrix} \sqrt{2} & 0 & 0 & \cdots & 0 \\ 0 & 1 & 0 & \cdots & 0 \\ 0 & 0 & 1 & \cdots & 0 \\ \vdots & \vdots & \vdots & \cdots & \vdots \\ 0 & 0 & 0 & \cdots & 1 \end{bmatrix} \begin{bmatrix} \frac{1}{\sqrt{2}} & \frac{1}{\sqrt{2}} & \frac{1}{\sqrt{2}} & \cdots & \frac{1}{\sqrt{2}} \\ \cos\theta_1 & \cos\theta_2 & \cos\theta_3 & \cdots & \cos\theta_n \\ \sin\theta_1 & \sin\theta_2 & \sin\theta_3 & \cdots & \sin\theta_n \\ \vdots & \vdots & \vdots & \cdots & \vdots \\ \cos(m\theta_1) & \cos(m\theta_2) & \cos(m\theta_3) & \cdots & \cos(m\theta_n) \\ \sin(m\theta_1) & \sin(m\theta_2) & \sin(m\theta_3) & \cdots & \sin(m\theta_n) \end{bmatrix}. \tag{A1}$$

Denote the last matrix by $\mathbf{B}$,

$$\mathbf{B} = \begin{bmatrix} \frac{1}{\sqrt{2}} & \frac{1}{\sqrt{2}} & \frac{1}{\sqrt{2}} & \cdots & \frac{1}{\sqrt{2}} \\ \cos\theta_1 & \cos\theta_2 & \cos\theta_3 & \cdots & \cos\theta_n \\ \sin\theta_1 & \sin\theta_2 & \sin\theta_3 & \cdots & \sin\theta_n \\ \vdots & \vdots & \vdots & \cdots & \vdots \\ \cos(m\theta_1) & \cos(m\theta_2) & \cos(m\theta_3) & \cdots & \cos(m\theta_n) \\ \sin(m\theta_1) & \sin(m\theta_2) & \sin(m\theta_3) & \cdots & \sin(m\theta_n) \end{bmatrix}, \tag{A2}$$

and due to the orthogonal property of $\mathbf{B}$ we have

$$\mathbf{B}\mathbf{B}^T = \frac{n}{2}\mathbf{I}_n, \tag{A3}$$

where $n = 2m+1$.

Let

$$\mathbf{C} = \frac{\sqrt{2}}{\sqrt{n}}\mathbf{B}, \tag{A4}$$

and then by Eq. (A3) we have

$$\mathbf{C}\mathbf{C}^T = \mathbf{I}_n. \tag{A5}$$

From this equation it follows that

$$\mathbf{C}^{-1} = \mathbf{C}^T = \frac{\sqrt{2}}{\sqrt{n}}\mathbf{B}^T. \tag{A6}$$

In terms of $\mathbf{C}$, we have

$$\mathbf{T}_\theta = \frac{\sqrt{n}}{\sqrt{2}} \begin{bmatrix} \sqrt{2} & 0 & 0 & \cdots & 0 \\ 0 & 1 & 0 & \cdots & 0 \\ 0 & 0 & 1 & \cdots & 0 \\ \vdots & \vdots & \vdots & \cdots & \vdots \\ 0 & 0 & 0 & \cdots & 1 \end{bmatrix} \mathbf{C}, \tag{A7}$$

and thus

$$\begin{aligned} \mathbf{T}_\theta^{-1} &= \frac{\sqrt{2}}{\sqrt{n}}\mathbf{C}^{-1} \begin{bmatrix} \frac{1}{\sqrt{2}} & 0 & 0 & \cdots & 0 \\ 0 & 1 & 0 & \cdots & 0 \\ 0 & 0 & 1 & \cdots & 0 \\ \vdots & \vdots & \vdots & \cdots & \vdots \\ 0 & 0 & 0 & \cdots & 1 \end{bmatrix} \\ &= \frac{2}{n}\mathbf{B}^T \begin{bmatrix} \frac{1}{\sqrt{2}} & 0 & 0 & \cdots & 0 \\ 0 & 1 & 0 & \cdots & 0 \\ 0 & 0 & 1 & \cdots & 0 \\ \vdots & \vdots & \vdots & \cdots & \vdots \\ 0 & 0 & 0 & \cdots & 1 \end{bmatrix}. \end{aligned} \tag{A8}$$

Inserting Eq. (A2) for $\mathbf{B}$ into the above equation we obtain

$$\mathbf{T}_\theta^{-1} = \frac{2}{n}$$

$$\begin{bmatrix} \frac{1}{2} & \cos\theta_1 & \sin\theta_1 & \cdots & \cos(m\theta_1) & \sin(m\theta_1) \\ \frac{1}{2} & \cos\theta_2 & \sin\theta_2 & \cdots & \cos(m\theta_2) & \sin(m\theta_2) \\ \vdots & \vdots & \vdots & \cdots & \vdots & \vdots \\ \frac{1}{2} & \cos\theta_n & \sin\theta_n & \cdots & \cos(m\theta_n) & \sin(m\theta_n) \end{bmatrix} \tag{A9}$$

Then, from Eq. (55) we can derive the inverse of **K** by

$$\mathbf{K}^{-1} = \frac{2}{n} \begin{bmatrix} \frac{1}{2\ln R} & -\frac{R}{R_0}\cos\theta_1 & -\frac{R}{R_0}\sin\theta_1 & \cdots \\ \frac{1}{2\ln R} & -\frac{R}{R_0}\cos\theta_2 & -\frac{R}{R_0}\sin\theta_2 & \cdots \\ \vdots & \vdots & \vdots & \cdots \\ \frac{1}{2\ln R} & -\frac{R}{R_0}\cos\theta_n & -\frac{R}{R_0}\sin\theta_n & \cdots \end{bmatrix} \begin{bmatrix} -\frac{mR^m}{R_0^m}\cos(m\theta_1) & -\frac{mR^m}{R_0^m}\sin(m\theta_1) \\ -\frac{mR^m}{R_0^m}\cos(m\theta_2) & -\frac{mR^m}{R_0^m}\sin(m\theta_2) \\ \vdots & \vdots \\ -\frac{mR^m}{R_0^m}\cos(m\theta_n) & -\frac{mR^m}{R_0^m}\sin(m\theta_n) \end{bmatrix}. \tag{A10}$$

References

Atluri, S. N.; Kim, H. G.; Cho, J. Y. (1999): A critical assessment of the truly meshless local Petrov-Galerkin (MLPG), and local boundary integral equation (LBIE) methods. *Computational Mechanics*, vol. 24, pp. 348-372.

Atluri, S. N.; Shen, S. (2002): The meshless local Petrov-Galerkin (MLPG) method: a simple & less-costly alternative to the finite element and boundary element methods. *CMES: Computer Modeling in Engineering and Sciences*, vol. 3, pp. 11-51.

Bogomolny, A. (1985): Fundamental solutions method for elliptic boundary value problems. *SIAM Journal on Numerical Analysis*, vol. 22, pp. 644-669.

Cao, Y.; Schultz, W. W.; Beck, R. F. (1991): Three-dimensional desingularized boundary integral methods for potential problems. *International Journal for Numerical Methods in Fluids*, vol. 12, pp. 785-803.

Chen, C. S.; Cho, H. A.; Golberg, M. A. (2006): Some comments on the ill-conditioning of the method of fundamental solutions. *Engineering Analysis with Boundary Elements*, vol. 30, pp. 405-410.

Chen, J. T.; Chang, M. H.; Chen, K. H.; Lin, S. R. (2002): The boundary collocation method with meshless concept for acoustic eigenanalysis of two-dimensional cavities using radial basis function. *Journal of Sound and Vibration*, vol. 257, pp. 667-711.

Chen, J. T.; Chang, M. H.; Chen, K. H.; Chen, I. L. (2002): Boundary collocation method for acoustic eigenanalysis of three-dimensional cavities using radial basis function. *Computational Mechanics*, vol. 29, pp. 392-408.

Chen J. T.; Wu C. S.; Lee Y. T.; Chen K. H. (2007): On the equivalence of the Trefftz method and method of fundamental solutions for Laplace and biharmonic equations. Computers and Mathematics with Applications 2007;53:851-879.

Chen, W.; Tanaka, M. (2002): A meshless, integration-free, and boundary-only RBF technique. *Computers and Mathematics with Applications*, vol. 43, pp. 379-391.

Cheng, R. S. C. (1987): Delta-trigonometric and spline methods using the single-layer potential representation. PhD Dissertation, University of Maryland.

Cho, H. A., Golberg, M. A.; Muleshkov, A. S.; Li, X. (2004): Trefftz methods for time-dependent partial differential equations. *CMC: Computers, Materials & Continua*, vol. 1, pp. 1-37.

Chuang, J. M. (1999): Numerical studies on desingularized Cauchy's formula with applications to interior potential problems. *International Journal for Numerical Methods in Engineering*, vol. 46, pp. 805-824.

Fairweather, G.; Karageorghis, A. (1998): The method of fundamental solutions for elliptic boundary value problems. *Advances in Computational Mathematics*, vol. 9, pp. 69-95.

Fan, C. M.; Young, D. L. (2002): Analysis of the 2D Stokes flows by the nonsingular boundary integral equation method. *International Mathematical Journal*, vol. 2, pp. 1199-1215.

Golberg, M. A.; Chen, C. S. (1996): Discrete Projection Methods for Integral Equations. Computational Mechanics Publications, Southampton.

Han, P. S.; Olson, M. D. (1987): An adaptive boundary element method. *International Journal for Numerical Methods in Engineering*, vol. 24, pp. 1187-1202.

Hon, Y. C.; Wei, T. (2005): The method of fundamental solution for solving multidimensional inverse heat conduction problems. *CMES: Computer Modeling in Engineering & Sciences*, vol. 7, pp. 119-132.

Hwang, W. S.; Huang, Y. Y. (1998): Nonsingular direct formulation of boundary integral equations for potential flows. *International Journal for Numerical Methods in Fluids*, vol. 26, pp. 627-635.

Jin, B.; Chen, W. (2006): Boundary knot method based on geodesic distance for anisotropic problems. *Journal of Computational Physics*, vol. 215, pp. 614-629.

Kita, E.; Kamiya, N. (1995): Trefftz method: an overview. *Advances in Engineering Software*, vol. 24, pp. 3-12.

Kita, E.; Kamiya, N.; Iio, T. (1999): Application of a direct Trefftz method with domain decomposition to 2D potential problems. *Engineering Analysis with Boundary Elements*, vol. 23, pp. 539-548.

Landweber, L.; Macagno, M. (1969): Irrotational flow about ship forms. IIHR Report No. 123, Iowa University.

Lalli, F. (1991): On the accuracy of the desingularized boundary integral method in free surface flow problems. *International Journal for Numerical Methods in Fluids*, vol. 25, pp. 1163-1184.

Li, Z. C.; Lu, T. T.; Huang, H. T.; Cheng, A. H. D. (2006): Trefftz, collocation, and other boundary methods–A comparison. *Numerical Methods for Partial Differential Equations*, vol. 23, pp. 93-144.

Liu, C.-S. (2007a): A modified Trefftz method for two-dimensional Laplace equation considering the domain's characteristic length. *CMES: Computer Modeling in Engineering & Sciences*, vol. 21, pp. 53-65.

Liu, C.-S. (2007b): A meshless regularized integral equation method for Laplace equation in arbitrary interior or exterior plane domains. *CMES: Computer Modeling in Engineering & Sciences*, vol. 19, pp. 99-109.

Liu, C.-S. (2007c): A MRIEM for solving the Laplace equation in the doubly-connected domain. *CMES: Computer Modeling in Engineering & Sciences*, vol. 19, pp. 145-161.

Liu, C.-S. (2007d): A highly accurate solver for the mixed-boundary potential problem and singular problem in arbitrary plane domain. *CMES: Computer Modeling in Engineering & Sciences*, vol. 20, pp. 111-122.

Liu, C.-S. (2007e): An effectively modified direct Trefftz method for 2D potential problems considering the domain's characteristic length. *Engineering Analysis with Boundary Elements*, vol. 31, pp. 983-993.

Liu, C.-S. (2008): A highly accurate collocation Trefftz method for solving the Laplace equation in the doubly connected domains. *Numerical Methods for Partial Differential Equations*, vol. 24, pp. 179-192.

Ramachandran, P. A. (2002): Method of fundamental solutions: singular value decomposition analysis. *Communications in Numerical Methods in Engineering*, vol. 18, pp. 789-801.

Saavedra, I.; Power, H. (2003): Multipole fast algorithm for the least-squares approach of the method of fundamental solutions for three-dimensional harmonic problems. *Numerical Methods for Partial Differential Equations*, vol. 19, pp. 828-845.

Smyrlis, Y. S.; Karageorghis, A. (2001): Some aspects of the method of fundamental solutions for certain harmonic problems. *Journal of Scientific Computing*, vol. 16, pp. 341-371.

Smyrlis, Y. S.; Karageorghis, A. (2003): Some aspects of the method of fundamental solutions for certain biharmonic problems. *CMES: Com-*

puter Modeling in Engineering and Sciences, vol. 4, pp. 535-550.

Smyrlis, Y. S.; Karageorghis, A. (2004): Numerical analysis of the MFS for certain harmonic problems. *M2AN Mathematical Modeling and Numerical Analysis*, vol. 38, pp. 495-517.

Tsai, C. C.; Lin, Y. C.; Young, D. L.; Atluri, S. N. (2006): Investigations on the accuracy and condition number for the method of fundamental solutions. *CMES: Computer Modeling in Engineering and Sciences*, vol. 16, pp. 103-114.

Young, S. A. (1999): A solution method for two-dimensional potential flow about bodies with smooth surfaces by direct use of the boundary integral equation. *Communications in Numerical Methods in Engineering*, vol. 15, pp. 469-478.

Young, D. L.; Chen, K. H.; Lee, C. W. (2005): Novel meshless method for solving the potential problems with arbitrary domain. *Journal of Computational Physics*, vol. 209, pp. 290-321.

Young, D. L.; Chen, K. H.; Chen, J. T.; Kao, J. H. (2007): A modified method of fundamental solutions with source on the boundary for solving Laplace equations with circular and arbitrary domains. *CMES: Computer Modeling in Engineering & Sciences*, vol. 19, pp. 197-222.

Young, D. L.; Ruan J. W. (2005): Method of fundamental solutions for scattering problems of electromagnetic waves. *CMES: Computer Modeling in Engineering & Sciences*, vol. 7, pp. 223-232.

Young, D. L.; Tsai, C. C.; Lin, Y. C.; Chen, C. S. (2006): The method of fundamental solutions for eigenfrequencies of plate vibrations. *CMC: Computers, Materials & Continua*, vol. 4, pp. 1-10.

Zhang, Y. L.; Yeo, K. S.; Khoo, B. C.; Chong, W. K. (1999): Simulation of three-dimensional bubbles using desingularized boundary integral method. *International Journal for Numerical Methods in Fluids*, vol. 31, pp. 1311-1320.